

---

# Pulsed-THz Characterization of Hg-Based, High-Temperature Superconductors

## Introduction

Superconductivity is still regarded as a very promising technology to be applied in high-performance electronics (e.g., Josephson junction digital circuits, ultrasensitive magnetometers) and optoelectronics (broadband x-ray-to-visible-light photodetectors, optical single-photon and photon-number-resolving detectors). The discovery of high-temperature superconductors (HTS's)<sup>1</sup> made those applications technically easier to achieve, at least from the cryogenics point of view, since most HTS's require only liquid nitrogen cooling. Among them, the  $\text{HgBa}_2\text{Ca}_{n-1}\text{Cu}_n\text{O}_{2n+2+\delta}$  (HBCCO, Hg-based) compound, with its record high superconducting critical temperature  $T_c$  of 134 K at ambient pressure,<sup>2</sup> has attracted special attention. However, it is a very complicated system and its complete understanding from the physics, chemistry, and materials science points of view is needed in order to overcome the technological barriers facing HBCCO, and HTS's in general, in their quest for widespread applications.

This work presents comprehensive studies of time-resolved dynamics of Cooper pairs and quasiparticles in Hg-based superconductors. Our experiments implement a femtosecond optical system to perform the time-domain spectroscopy (TDS), using either pulses with 1-THz bandwidth for transmission measurements or the ultrafast optical-pump THz-probe (OTPT) characterization method. In the case of the transmission-type THz-TDS experiments, our sample is put into the path of a subpicosecond-in-duration, THz radiation burst and the transmitted electric-field waveform is measured. After performing the fast Fourier transform (FFT) of the time-domain transient, the frequency-dependent magnitude and phase components of the signal are obtained. By comparing the obtained data to the reference signal collected without the sample present in the system, either the frequency-dependent complex index of refraction  $n(\omega)$  or conductivity  $\sigma(\omega)$  of the sample's material can be deduced without resorting to Kramers–Kronig analysis. Since various pairing theories predict the different temperature behavior of the complex  $\sigma = \sigma_{\text{re}} - i\sigma_{\text{im}}$  in HTS's,<sup>3</sup> by measuring the temperature- and frequency-dependent components of  $\sigma$  ( $\sigma_{\text{re}}$  and  $\sigma_{\text{im}}$ ), we are able to provide insight

on the intrinsic relaxation dynamics of quasiparticles in the HBCCO material.

## Sample Fabrication and Experimental Setup

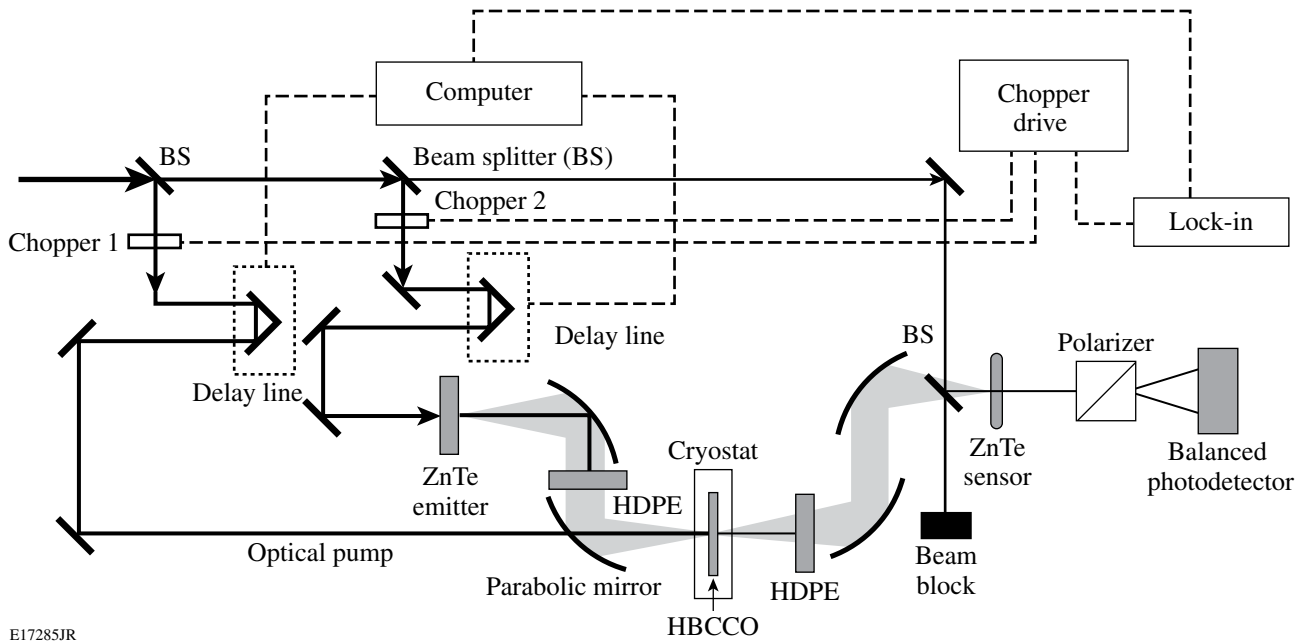
### 1. Sample Fabrication

Our Hg-based thin films were synthesized from 200 to 600-nm-thick Re-Ba-Ca-Cu-O precursor films, rf-magnetron sputtered at the room temperature on  $\text{LaAlO}_3$  substrates, then followed by an *ex-situ* mercuration process in a sealed, evacuated quartz ampoule, using an un-reacted (Hg, Re)-1223 pellet as the source of mercury, prepared by a sol-gel method. The ampoule was placed inside a furnace, kept at 800°C for 5 h, and later cooled at a rate of 120°C/h to the ambient temperature.<sup>4</sup>

The x-ray-diffraction analyses demonstrated that our films were predominantly composed of a *c*-axis-oriented Hg-1212 phase, together with a Hg-1223 phase. Four-point resistance measurements of chemically etched, 20- $\mu\text{m}$ -wide microbridges, showed that the samples used in this study exhibited the onset of the superconducting transition  $T_{c,\text{on}}$  at  $\sim 122$  K and the zero-resistance  $T_{c,0}$  at  $\sim 110$  K.<sup>4</sup>

### 2. Experimental Setup

Figure 116.49 shows our experimental setup. A 1-kHz, 800-nm-wavelength, 50-fs-duration commercial Ti:sapphire amplifier system was used as a laser source with a total output of  $\sim 500$  mW. The output from the laser was split into three beams: one beam was used to optically pump the Hg-based sample and generate photoexcited quasiparticles; the second beam was used to generate THz radiation via optical rectification in a ZnTe emitter; and the third one (very weak) detected the THz transmission signal via a free-space, electro-optic sampling in a ZnTe sensor. The generated THz transient was formed and focused on the HBCCO sample (marked by an arrow in Fig. 116.49) using two sets of metallic parabolic mirrors. The sample was mounted on a cold finger inside an optical, continuous-flow, liquid-helium cryostat with the temperature controlled between 8 K and 293 K. The computer-based data-acquisition system monitored current flow through two balanced photodetectors using a lock-in amplifier. The



E17285JR

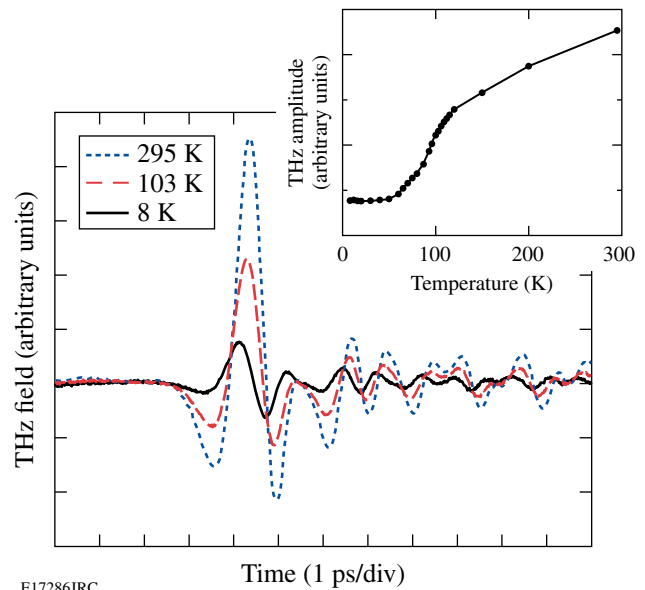
Figure 116.49  
THz-TDS/OPTP experimental setup.

same setup was used for both the transmission THz-TDS and OPTP measurements, but, of course, the optical pump beam was blocked when performing transmission THz-TDS experiments. Further technical details of the experimental setup and OPTP spectroscopy can be found in Ref. 5.

## Experimental Results and Discussion

### 1. THz-TDS Experiments

The transmission THz-TDS experiments were performed in the temperature range between 8 K and 293 K on both the HBCCO thin film and the bare  $\text{LaAlO}_3$  substrate. Figure 116.50 shows the transmitted THz signals for a nominally (before annealing) 500-nm-thick HBCCO film at different temperatures. The THz transient amplitude decreases and the peak position slightly shifts as the temperature drops below  $T_c$ , indicating that Cooper pairs contribute to both the increased reflectivity and the phase shift via the imaginary component of the conductivity. We stress that the observed temperature-related changes in the THz transient are solely due to the change in the HBCCO superconducting properties since the reference THz-TDS studies performed on the bare  $\text{LaAlO}_3$  did not reveal any changes, indicating no substrate absorption. The refractive index of  $\text{LaAlO}_3$  remained constant and was  $\sim 4.85$  for frequencies below 1 THz, which agrees with the results reported by Zhang.<sup>6</sup> As shown in the inset in Fig. 116.50, above  $T_c$ , the amplitude of the transmitted electric field decreased slowly with



E17286JRC

Figure 116.50  
Transmitted THz field through a HBCCO film at different temperatures. The inset shows temperature dependence of the THz field amplitude.

the temperature decrease, due to the progressive increase of the film's conductivity. When the temperature crossed  $T_c$ , there was a sharp drop in the THz transmission, as we will show later, directly related to the strong increase in  $\sigma_{im}$ .

## 2. THz-TDS Experiments—Complex Conductivity Analysis

Our HBCCO film on the  $\text{LaAlO}_3$  substrate was put in the experimental THz optical path at the normal incidence to the THz beam as is schematically illustrated in Fig. 116.51(a). Therefore, the transmitted waveform can be expressed as

$$E_{\text{sam+sub}} = Et(\omega)t_{31}\exp[in_3(\omega/c)d_3], \quad (1)$$

with the transmission coefficient  $t$  of the air/HBCCO/ $\text{LaAlO}_3$  system equal to<sup>7</sup>

$$t(\omega) = \frac{t_{12}t_{23}\exp[in_2(\omega/c)d_2]}{1 + r_{12}r_{23}\exp[2in_2(\omega/c)d_2]}, \quad (2)$$

where  $t_{ij} = 2n_i/(n_i + n_j)$ ,  $r_{ij} = (n_i - n_j)/(n_i + n_j)$ ,  $E$  is the incident THz field,  $d_2$  and  $d_3$  are thicknesses of the thin film and the substrate, respectively, and  $n_i$  and  $n_j$  are complex refraction indexes. In general, we should consider a Fabry–Pérot effect due to multiple reflections from the interferences.<sup>8</sup> However, the thickness of  $\text{LaAlO}_3$  is  $\sim 0.5$  mm, so even the first-reflection signal is going to be outside the time window of interest associated with the transmitted signal; therefore, reflections can be ignored.

In the case of the bare  $\text{LaAlO}_3$  substrate illuminated with the THz radiation [Fig. 116.51(b)], the transmitted waveform can be expressed as

$$E_{\text{air+sub}} = Et_{13}t_{31}\exp[in_3(\omega/c)d_3]\exp[i(\omega/c)d_2]. \quad (3)$$

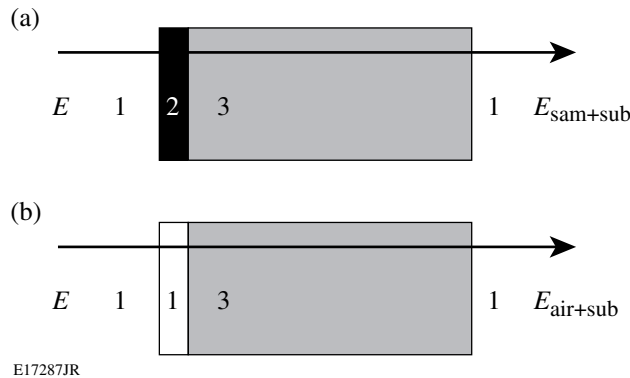


Figure 116.51 Schematic of THz wave transmission through (a) an HBCCO thin-film sample +  $\text{LaAlO}_3$  substrate (sam+sub) and (b) air + a bare  $\text{LaAlO}_3$  substrate (air+sub). The numbers 1, 2, and 3 correspond to air, HBCCO sample, and  $\text{LaAlO}_3$  substrate, respectively.

Thus, dividing Eqs. (1) and (3), we get

$$\begin{aligned} \frac{E_{\text{sam+sub}}}{E_{\text{air+sub}}} &= t(\omega)/\{t_{13}\exp[i(\omega/c)d_2]\} \\ &= A(\omega)\exp[i\phi(\omega)], \end{aligned} \quad (4)$$

where  $A(\omega)$  is the frequency-dependent magnitude of  $E_{\text{sam+sub}}$  divided by that of  $E_{\text{air+sub}}$ , and  $\phi(\omega)$  is the frequency-dependent phase of  $E_{\text{sam+sub}}$  subtracted by that of  $E_{\text{air+sub}}$ . Since, in our case,  $|n_2(\omega/c)d| \ll 1$ , and  $|n_2| \gg n_3 \gg 1$ , therefore<sup>7</sup>

$$\frac{1 + n_3}{1 + n_3 Z_0 d_2 \sigma(\omega)} = A(\omega)\exp\{i[\phi(\omega) + \omega d_2/c]\}, \quad (5)$$

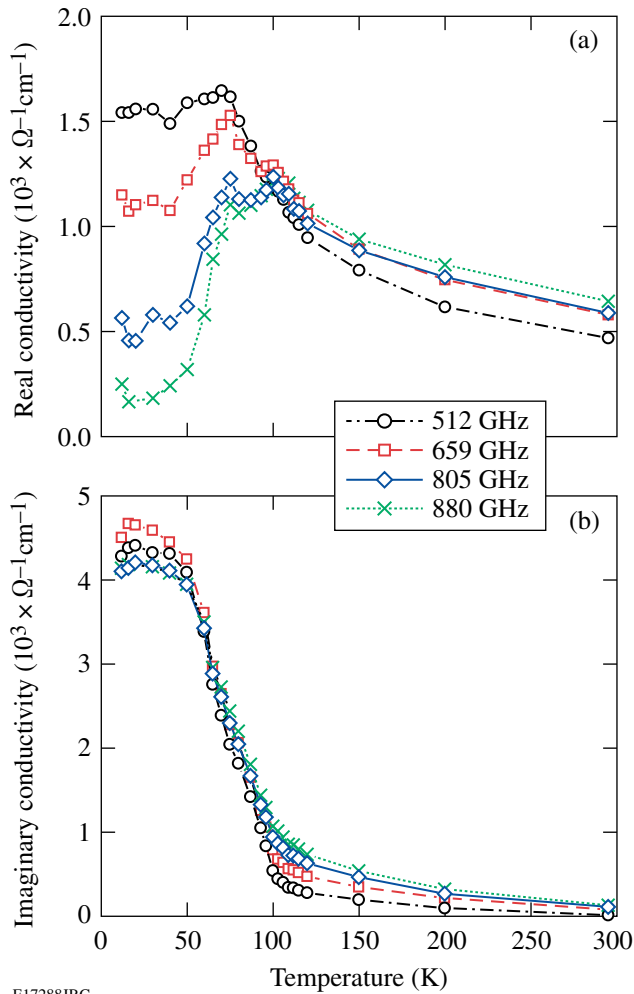
where  $Z_0$  is the impedance of free space. Equation (5) shows that now we can directly relate the experimentally measured THz-TDS spectra given by Eq. (4) to the tested complex  $\sigma(\omega)$  of our sample.

The complex  $\sigma(\omega)$  of superconductors can be described by the two-fluid model<sup>1</sup> and is composed of two parts: (1) an imaginary part that is dominant below  $T_c$  and related to the superfluid fraction  $f_s$  of electrons and (2) a Drude component proportional to the quasiparticle (normal electron) fraction  $f_n$  (Ref. 3):

$$\sigma(\omega, T) = \sigma_{\text{re}} + i\sigma_{\text{im}} = \frac{ne^2}{m^*} \left[ \frac{f_n(T)}{\tau(\omega, T)^{-1} - i\omega} - \frac{f_s(T)}{i\omega} \right], \quad (6)$$

where  $f_n + f_s = 1$  and  $\tau(\omega, T)$  is the quasiparticle scattering time.

The temperature dependences of  $\sigma_{\text{re}}$  and  $\sigma_{\text{im}}$  are presented in Fig. 116.52. Figure 116.52(a) shows that  $\sigma_{\text{re}}$  increases with the decrease of temperature, exhibits a small cusp at  $\sim T_c$ , and reaches the main peak below  $T_c$ , which is due to a competition of the quasiparticle density decrease and simultaneous increase of their scattering rate. The main  $\sigma_{\text{re}}$  peak [see Fig. 116.52(a)] shifts to lower temperatures with lower frequencies, and its amplitude becomes larger. On the other hand, Fig. 116.52(b) demonstrates that the  $\sigma_{\text{im}}$  component increases dramatically below  $T_c$ , which is due to the presence and increase of the superconducting condensate (Cooper pairs). There is a small nonzero  $\sigma_{\text{im}}$  in the normal state, apparently due to a residual kinetic-inductive effect. The latter can be speculated as evidence of the pseudogap state, but more systematic studies are needed.



E17288JRC

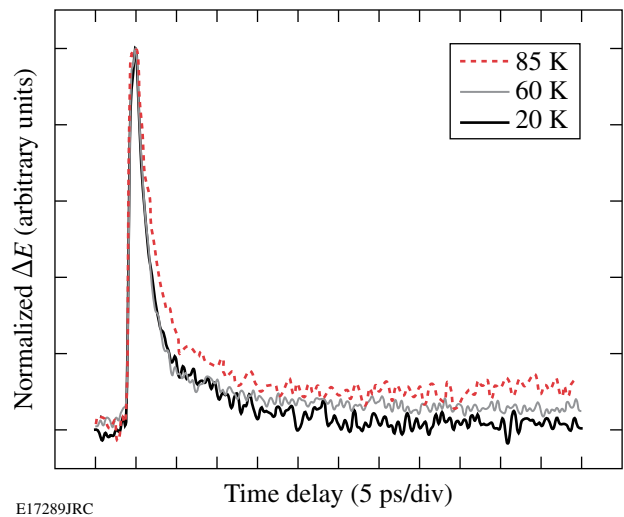
Figure 116.52

(a) Temperature-dependent real conductivity at different frequencies; (b) temperature-dependent imaginary conductivity at different frequencies.

### 3. Time-Resolved OPTP Experiments

Optical excitation of a superconductor induces  $\Delta\sigma_{\text{re}}$  and  $\Delta\sigma_{\text{im}}$  changes, which result in a change of the transmitted transient THz electric field  $\Delta E(t)$ . As we mentioned before, the  $\Delta\sigma_{\text{im}}$  component contains information about the superconducting condensate density, while the quasiparticle (normal electron) density is probed by  $\Delta\sigma_{\text{re}}$ . In our OPTP measurements, optical excitation increases the amplitude of the transient THz signal. Thus, we can fix the THz-probe-signal optical-delay line at the position where the positive, maximum peak of the THz electric-field waveform occurs [ $\Delta E(t = t_{\text{max}})$ ] and, subsequently, vary the arrival time of the femtosecond optical excitation pump pulse (see Fig. 116.49). This way we can obtain the time-resolved  $\Delta\sigma(t)$  dynamics and the corresponding quasiparticle dynamics.

Figure 116.53 shows our OPTP results at different temperatures below  $T_c$  with an optical fluence of the pump beam equal to  $2 \mu\text{J}/\text{cm}^2$ . The measured THz  $\Delta E(t)$  transients have their decay times of the order of 2 ps and represent the quasiparticle relaxation (Cooper-pair formation) dynamics. We note that the above observation is contrary to the common, slow relaxation process in photoinduced superconductors, typical for conventional (e.g., metallic) superconductors, where the quasiparticle relaxation speed is limited by the acoustic-phonon escape time for the film to the substrate. The latter is called the phonon-bottleneck effect<sup>9</sup> and is due to the secondary pair-breaking by the acoustic phonons emitted during the process of two-quasiparticle recombination into a Cooper pair. The corresponding phonon escape time is in the nanosecond range, depending linearly on the superconductor thickness. In HBCCO superconductors,  $2\Delta$  is estimated to be in the 50- to 70-meV range and the acoustic phonons predominantly relax enharmonically; thus, they are decoupled from the carriers, resulting in the direct intrinsic quasiparticle recombination process. According to Fig. 116.53, far below  $T_c$ , our HBCCO material relaxes back to the fully superconducting (equilibrium) state in less than 2 ps. The latter observation is in direct agreement with our earlier, all-optical, pump-probe spectroscopy studies<sup>10</sup> and confirms that, far below  $T_c$ , thermal (phonon) contribution is negligible in the relaxation dynamics of the nonequilibrium HBCCO superconductors.



E17289JRC

Figure 116.53

Normalized transient transmitted electrical field signals at different temperatures below  $T_c$  obtained from OPTP experiments.

## Conclusion

We presented our complex conductivity studies of HBCCO HTS thin films using the THz-TDS and OPTP techniques. THz studies are the volume measurements; thus, they are insensitive to the sample roughness or granularity, which are much smaller in size compared to the THz radiation wavelength. The latter is important in the case of our *ex-situ*-grown HBCCO films, which have a rough surface and are to some extent multi-phased specimens. From the transient THz transmission measurements, one observed that  $\Delta\sigma_{\text{re}}$  shows a peak below  $T_c$ , which shifts to lower temperatures with lower frequencies. At the same time,  $\Delta\sigma_{\text{im}}$  has a sharp increase below  $T_c$  due to the increase in Cooper-pair density and formation of a superconducting condensate. Both findings are in general agreement with the complex conductivity model for low-energy excitations (far below the material's  $2\Delta$ ) in superconductors. The time-resolved quasiparticle relaxation of HBCCO, measured directly by the OPTP techniques, exhibits an intrinsic single-picosecond dynamics with no phonon bottleneck, or a substantial bolometric signal plateau, which is a unique feature among both LT and HT nonequilibrium superconductors, and makes this material very promising for ultrafast photodetector applications.

## ACKNOWLEDGMENT

This work was supported by the US AFOSR grant FA9550-06-1-0348 (Rochester), the Slovak Research and Development Support Agency grants 2/0139/08 and LPP-0078-07 (Bratislava), and the NSF Center on Materials and Devices for Information Technology Research (CMDITR), DMR-0120967 (Baltimore).

## REFERENCES

1. See, e.g., M. Tinkham, *Introduction to Superconductivity*, 2nd ed., International Series in Pure and Applied Physics (McGraw-Hill, New York, 1996), pp. 108–381.
2. C. W. Chu, *Chin. J. Phys.* **34**, 166 (1996).
3. R. D. Averitt *et al.*, *J. Opt. Soc. Am. B* **17**, 327 (2000).
4. Š. Chromik, M. Valeriánová, V. Štrbík, Š. Gaži, P. Odier, X. Li, Y. Xu, R. Sobolewski, F. Hanic, G. Plesch, and Beňačka, *Appl. Surf. Sci.* **254**, 3638 (2008).
5. P. D. Cunningham and L. M. Hayden, *J. Phys. Chem.* **112**, 7928 (2008).
6. Z. M. Zhang *et al.*, *J. Opt. Soc. Am. B* **11**, 2252 (1994).
7. T.-R. Tsai, C.-C. Chi, and S.-F. Horng, *Physica C* **391**, 281 (2003).
8. L. Duvillaret, F. Garet, and J.-L. Coutaz, *IEEE J. Sel. Top. Quantum Electron.* **2**, 739 (1996).
9. A. Rothwarf and B. N. Taylor, *Phys. Rev. Lett.* **19**, 27 (1967).
10. X. Li, Y. Xu, Š. Chromik, V. Štrbík, P. Odier, D. De Barros, and R. Sobolewski, *IEEE Trans. Appl. Supercond.* **15**, 622 (2005).